



## Natural Convection in Trapezoidal Enclosure Heated Partially from Below

Ahmed W. Mustafa\* Ihsan Ali Ghani\*\*

\*Department of Mechanical Engineering/College of Engineering/University of Tikrit

\*\*Department of Mechanical Engineering/College of Engineering/University of Al-Mustansiriya

\*E-mail: [ahmedweh@yahoo.com](mailto:ahmedweh@yahoo.com)

\*\*E-mail: [iaghani68@yahoo.com](mailto:iaghani68@yahoo.com)

(Received 20 July 2011; Accepted 22 November 2011)

### Abstract

Natural convection in a trapezoidal enclosure with partial heating from below and symmetrical cooling from the sides has been investigated numerically. The heating is simulated by a centrally located heat source on the bottom wall, and four different values of the dimensionless heat source length, 1/5, 2/5, 3/5, 4/5 are considered. The laminar flow field is analyzed numerically by solving the steady, two-dimensional incompressible Navier-Stokes and energy equations. The Cartesian velocity components and pressure on a collocated (non-staggered) grid are used as dependent variables in the momentum equations discretized by finite volume method; body fitted coordinates are used to represent the trapezoidal enclosure, and grid generation technique based on elliptic partial differential equations is employed. SIMPLE algorithm is used to adjust the velocity field to satisfy the conservation of mass. The range of Rayleigh number is ( $10^3 \leq Ra \leq 10^5$ ) and Prandtl number is 0.7. The results show that the average Nusselt number increases with the increases of the source length.

**Keywords:** Natural Convection, Trapezoidal Enclosure, Finite Volume.

### 1. Introduction

In recent years, an ever-increasing awareness in thermally driven flows reflects that fluid motions and transport processes generated or altered by buoyancy force are of interest due to the practical significances in many fields of science and technology. As a result, this subject is currently studied in diverse areas of meteorology, geophysics, energy storage, fire control, studies of air movement in attics and greenhouses, solar distillers, growth of crystals in liquids, etc.

Iyican and Bayazitoglu (1980) investigated natural convective flow and heat transfer within a trapezoidal enclosure with parallel cylindrical top and bottom walls at different temperatures and plane adiabatic side walls. The flow features in trapezoidal enclosures are predicted using data collected for rectangular enclosures. Peric (1993) studied natural convection in a trapezoidal cavities with a series of systematically refined

grids from 10 X 10 to 160 X 160 control volume and observed the convergence of results for grid independent solutions. Kuyper and Hoogendoorn (1995) investigated laminar natural convection flow in trapezoidal enclosures to study the influence of the inclination angle on the flow and also the dependence of the average Nusselt number on the Rayleigh number. Natarajan etc. (2008) investigated natural convection within a trapezoidal enclosure with uniform and non-uniform heating of the bottom wall of the enclosure, they found that the non-uniform heating of the bottom wall produces greater heat transfer rate at the center of the bottom wall than uniform heating case for all Rayleigh numbers but average Nusselt number shows an overall lower heat transfer rate for non-uniform heating case.

Basak etc. (2009) investigated laminar natural convection inside trapezoidal with uniform and non-uniform heated bottom wall, insulated top wall and isothermal sides with inclination angle

(40°, 30°, 0°)and for range of Rayleigh( $10^3 \leq Ra \leq 10^5$ ) and Prandtl number(  $0.026 \leq Pr \leq 1000$ ).They found that the average heat transfer does not vary significantly with angles for non-uniform heating of bottom wall .

It is seen from the literature that no attempt has been made for the detailed calculations of local and average Nusselt numbers on a natural convection flow within a trapezoidal enclosure for partial heating.

Symmetrical cooling from the sides is expected to be an efficient cooling option, while partial heating at the lower surface simulates the electronic components such as chips. The present study deals with a natural convection flow within a trapezoidal enclosure where the bottom wall is partially heated and vertical walls are cooled by means of a constant temperature bath whereas the top wall is well insulated.

## 2. Problem Formulation

Consider the motion of a viscous fluid within a trapezoidal enclosure with equal base length and height,  $L = H$  with the left wall inclined at an angle  $\phi = 30^\circ$  and with the y-axis as shown in Figure (1a). The bottom wall has a centrally located heat source of length (E) which is assumed to be isothermally heated at temperature ( $T_h$ ), the sidewalls are isothermally cooled at a constant temperature ( $T_c$ ); while the bottom surface, except for the heated section, and the upper wall is considered to be adiabatic. The fluid properties are assumed constant except for the density variation which is treated according to Boussinesq approximation. The present flow is considered steady,laminar, incompressible and two-dimensional. The viscous incompressible flow and the temperature distribution inside the enclosure are described by the Navier–Stokes and the energy equations, respectively (Bejan [6], 1993):

$$\frac{\partial u}{\partial x} + \frac{\partial v}{\partial y} = 0 \quad \dots(1)$$

$$u \frac{\partial u}{\partial x} + v \frac{\partial u}{\partial y} = -\frac{1}{\rho} \frac{\partial p}{\partial x} + \nu \left[ \frac{\partial^2 u}{\partial x^2} + \frac{\partial^2 u}{\partial y^2} \right] \quad \dots(2)$$

$$u \frac{\partial v}{\partial x} + v \frac{\partial v}{\partial y} = -\frac{1}{\rho} \frac{\partial p}{\partial y} + \nu \left[ \frac{\partial^2 v}{\partial x^2} + \frac{\partial^2 v}{\partial y^2} \right] + g\beta(T - T_c) \quad \dots(3)$$

$$u \frac{\partial T}{\partial x} + v \frac{\partial T}{\partial y} = \alpha \left[ \frac{\partial^2 T}{\partial x^2} + \frac{\partial^2 T}{\partial y^2} \right] \quad \dots(4)$$

The governing equations were transformed into dimensionless forms upon incorporating the following non-dimensional variables (Bejan[6], 1993):

$$X = \frac{x}{H}, \quad Y = \frac{y}{H}, \quad U = \frac{uH}{\alpha}, \quad V = \frac{vH}{\alpha},$$

$$\theta = \frac{T - T_c}{T_h - T_c}, \quad P = \frac{pH^2}{\rho\alpha^2}, \quad Pr = \frac{\nu}{\alpha},$$

$$Ra = \frac{g\beta(T_h - T_c)H^3 Pr}{\nu^2} \quad \dots(5)$$

Where X and Y are the dimensionless coordinates measured along the horizontal and vertical axes, respectively; u and v are the dimensional velocity components along x- and y axes, and  $\theta$  is the dimensionless temperature. The dimensionless forms of the governing equations under steady state condition are expressed in the following forms:

$$\frac{\partial U}{\partial X} + \frac{\partial V}{\partial Y} = 0 \quad \dots(6)$$

$$\frac{\partial U^2}{\partial X} + \frac{\partial UV}{\partial Y} = -\frac{\partial P}{\partial X} + Pr \left( \frac{\partial^2 U}{\partial X^2} + \frac{\partial^2 U}{\partial Y^2} \right) \quad \dots(7)$$

$$\frac{\partial UV}{\partial X} + \frac{\partial V^2}{\partial Y} = -\frac{\partial P}{\partial Y} + Pr \left( \frac{\partial^2 V}{\partial X^2} + \frac{\partial^2 V}{\partial Y^2} \right) + Ra Pr \theta \quad \dots(8)$$

$$\frac{\partial U\theta}{\partial X} + \frac{\partial V\theta}{\partial Y} = \left( \frac{\partial^2 \theta}{\partial X^2} + \frac{\partial^2 \theta}{\partial Y^2} \right) \quad \dots(9)$$

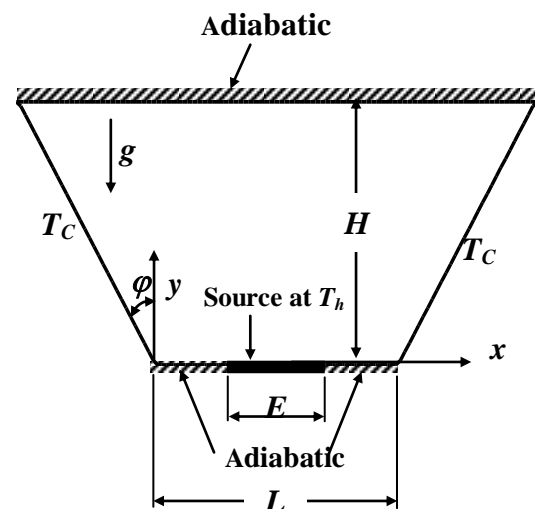


Fig.1a. Schematic Diagram of the Physical System.

### 3. Boundary Conditions

Boundary conditions can be summarized by the following equations:

Bottom Wall

$$\text{For all wall } \left( U = V = 0, \frac{\partial P}{\partial n} = 0 \right)$$

$$\text{but for adiabatic portion } \left( \frac{\partial \theta}{\partial n} = 0 \right)$$

and for source ( $\theta = 1$ )

Top Wall

$$U = V = 0, \frac{\partial \theta}{\partial n} = 0, \frac{\partial P}{\partial n} = 0$$

Left Wall

$$U = V = \theta = 0, \frac{\partial P}{\partial n} = 0$$

Right Wall

$$U = V = \theta = 0, \frac{\partial P}{\partial n} = 0$$

Where  $n$  is the normal direction on the walls.

### 4. Grid Generation and Numerical Solution

The set of conservation equations (6-9) can be written in general form in Cartesian coordinates as

$$\frac{\partial(U\phi)}{\partial X} + \frac{\partial(V\phi)}{\partial Y} = \frac{\partial}{\partial X} \left( \Gamma \frac{\partial \phi}{\partial X} \right) + \frac{\partial}{\partial Y} \left( \Gamma \frac{\partial \phi}{\partial Y} \right) + S_\phi \quad \dots(10)$$

Where  $\Gamma$  is the effective diffusion coefficient,  $\phi$  is the general dependent variable,  $S_\phi$  is the source term. The continuity equation (6) has no diffusion and source terms; it will be used to derive an equation for the pressure correction.

The grid generation scheme based on elliptic partial differential equations is used in the present study to generate the curvilinear coordinates. In this method, the curvilinear coordinates are generated by solving the following elliptic equations, (Thompson etc.[7], 1985)

$$\left. \begin{aligned} \alpha \frac{\partial^2 X}{\partial \zeta^2} - 2\gamma \frac{\partial^2 X}{\partial \zeta \partial \eta} + \beta \frac{\partial^2 X}{\partial \eta^2} &= 0 \\ \alpha \frac{\partial^2 Y}{\partial \zeta^2} - 2\gamma \frac{\partial^2 Y}{\partial \zeta \partial \eta} + \beta \frac{\partial^2 Y}{\partial \eta^2} &= 0 \end{aligned} \right\} \quad \dots(11)$$

Where  $\alpha, \beta, \gamma$  are the coefficients of transformation. They are expressed as

$$\alpha = \left( \frac{\partial X}{\partial \eta} \right)^2 + \left( \frac{\partial Y}{\partial \eta} \right)^2, \quad \gamma = \left( \frac{\partial X}{\partial \zeta} \frac{\partial X}{\partial \eta} \right) + \left( \frac{\partial Y}{\partial \zeta} \frac{\partial Y}{\partial \eta} \right),$$

$$\beta = \left( \frac{\partial X}{\partial \zeta} \right)^2 + \left( \frac{\partial Y}{\partial \zeta} \right)^2 \quad \dots(12)$$

The grid generation for the trapezoidal enclosure for number of control volume (30 X100) is illustrated in Figure (1b).

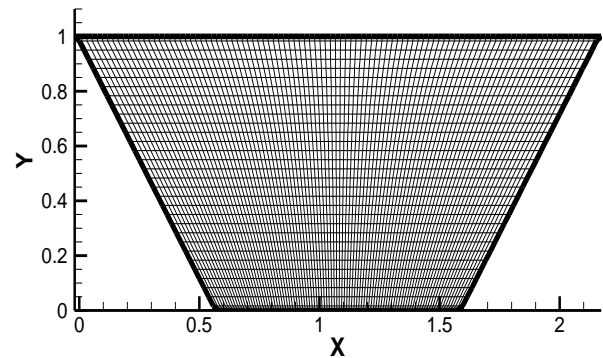


Fig.1b. Grid Generation for Number of Control Volumes MXN= 30X100

Equation (10) can be transformed from physical domain to computational domain according to the following transformation

$$\zeta = \zeta(X, Y), \quad \eta = \eta(X, Y),$$

The final form of the transformed equation can be written as:-

$$\frac{\partial}{\partial \zeta} (\phi G_1) + \frac{\partial}{\partial \eta} (\phi G_2) = \frac{\partial}{\partial \zeta} \left( \frac{\Gamma}{J} \left( \alpha \frac{\partial \phi}{\partial \zeta} - \gamma \frac{\partial \phi}{\partial \eta} \right) \right) + \frac{\partial}{\partial \eta} \left( \frac{\Gamma}{J} \left( \beta \frac{\partial \phi}{\partial \eta} - \gamma \frac{\partial \phi}{\partial \zeta} \right) \right) + JS_\phi \quad \dots(13)$$

Where  $G_1$  and  $G_2$  are the contra variant velocity components,  $J$  is the Jacobian of the transformation, on the computational plane. They are expressed as

$$G_1 = U \frac{\partial Y}{\partial \eta} - V \frac{\partial X}{\partial \eta}, \quad G_2 = V \frac{\partial X}{\partial \zeta} - U \frac{\partial Y}{\partial \zeta},$$

$$J = \left( \frac{\partial X}{\partial \zeta} \frac{\partial Y}{\partial \eta} - \frac{\partial Y}{\partial \zeta} \frac{\partial X}{\partial \eta} \right) \quad \dots(14)$$

The transferred equation (13) is integrated over the control volume in the computation domain. The convective terms are discretized by using hybrid scheme, while the diffusion terms are discretized by central scheme. SIMPLE algorithm on a collocated nonorthogonal grid is used to adjust the velocity field to satisfy the conservation of mass. Since all variables are stored in the center of the control volume, the interpolation method is used in the pressure correction equation to avoid the decoupling between velocity and pressure as in Rhie and Chow (1983). In order to consider the effect of the cross derivatives and to avoid solving a nine diagonal matrix of the pressure-correction equation, the cross derivatives are calculated by the approximate method of Wang and Komori (2000). The resulting set of discretization equations are solved iteratively using the line-by-line procedure which uses the Tri-Diagonal Matrix Algorithm (TDMA). The convergence criterion is that the maximum residuals in all equations fall below  $10^{-4}$ . For further information, numerical details can be found in Ferziger and Peric (1996).

**5. Grid Independence Test**

Computations have carried out for three selected grid sizes (i.e.,  $80 \times 30$ ,  $100 \times 40$ , and  $100 \times 50$ ). Figure (2) shows local Nusselt number distribution along the hot bottom wall for  $Ra = 10^6$  and  $e = 3/5$ . Results for the selected grid sizes show very good agreement with each other. Medium grid ( $100 \times 40$ ) is presented throughout this paper.

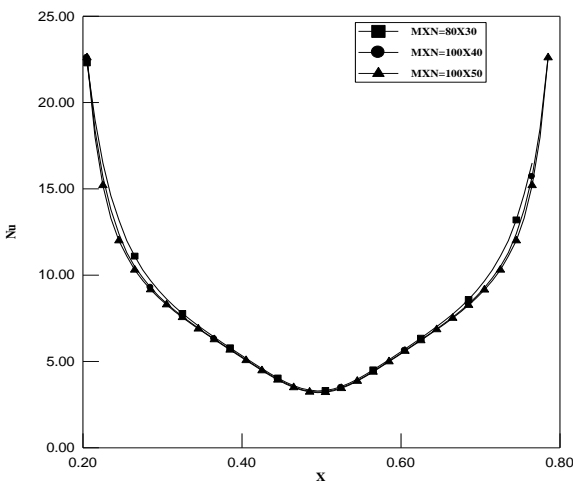


**Fig.2. Grid Independence Test for Local Nusselt Number for  $Ra = 10^5$ ,  $e = 3/5$ .**

**6. Validation**

The model validation is an essential part of a numerical investigation. Hence, the present numerical results are compared with the numerical results of Tanmay Basak etc. (2009), which were reported for laminar natural convection heat transfer in a trapezoidal enclosure heated isothermally from below while the other vertical walls are maintained at constant cold temperature and the top wall is well insulated, they solved the governing equations by using finite elements method. The comparison is conducted while employing the following dimensionless parameters:  $Ra = 10^5$ ,  $Pr = 0.7$  and trapezoidal angle  $\phi = 30^\circ$ . Excellent agreement is achieved, as illustrated in Figure (3), between the present results and the numerical results of Tanmay Basak etc. (2009).for the local Nusselt number distribution along the bottom wall.

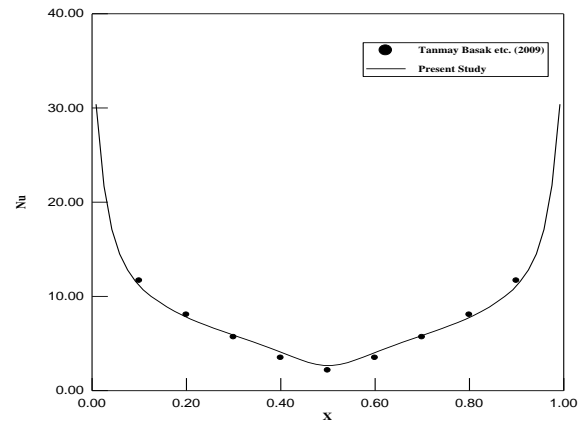


**Fig.3. Comparison of the Present Study with the Result of Tanmay Basak etc.(2009) for local Nusselt Number on the Bottom Wall of Trapezoidal Enclosure for  $Ra =10^5$ ,  $Pr = 0.7$  and Trapezoidal angle ( $\phi =30^\circ$ )**

**7. Results and Discussion**

Figures 4,5,6, and 7 show the effect of changing Rayleigh number for  $10^3 \leq Ra \leq 10^5$  and the effect of changing the dimensionless length of the heat source for  $e = (E/L) = 1/5, 2/5, 3/5,$  and  $4/5$  respectively, as in Aydin and Yang[11], (2000). Owing to the symmetrical boundary conditions on the side walls, the flow and temperature fields are symmetrical about the mid-length of the enclosure. The symmetrical boundary conditions in the vertical direction result in a pair of contour rotating cells on the left and right halves of the enclosure.

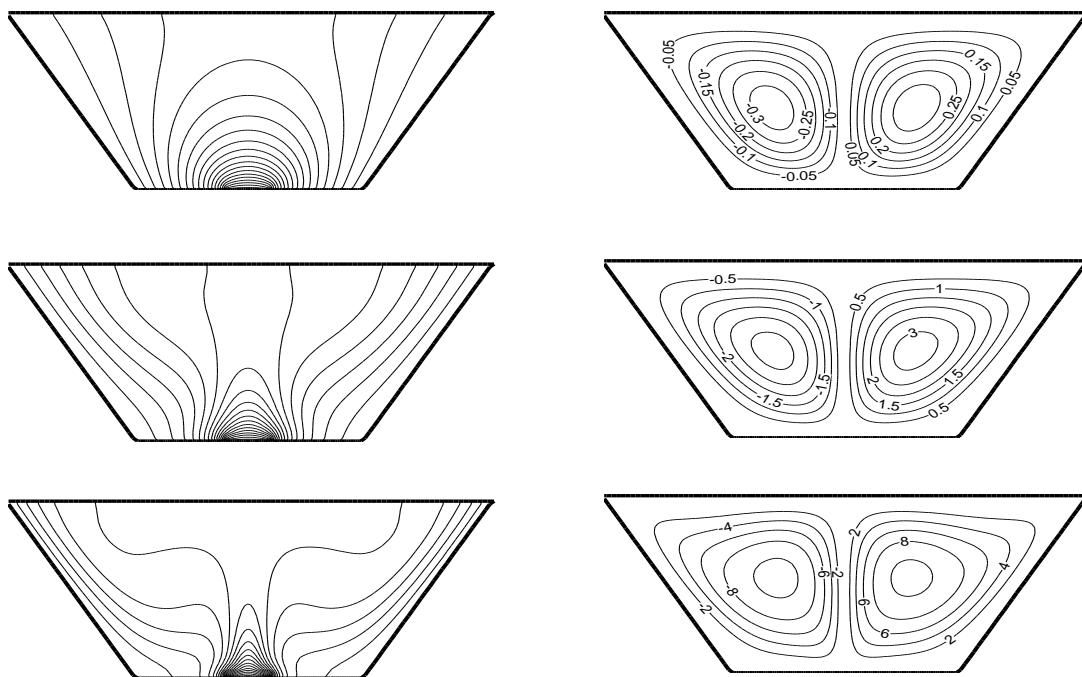


Fig.4. Isotherms (left) and Streamlines (right) for  $e = 1/5$  and (a)  $Ra = 10^3$  , (b)  $Ra = 10^4$  , (c)  $Ra = 10^5$ .

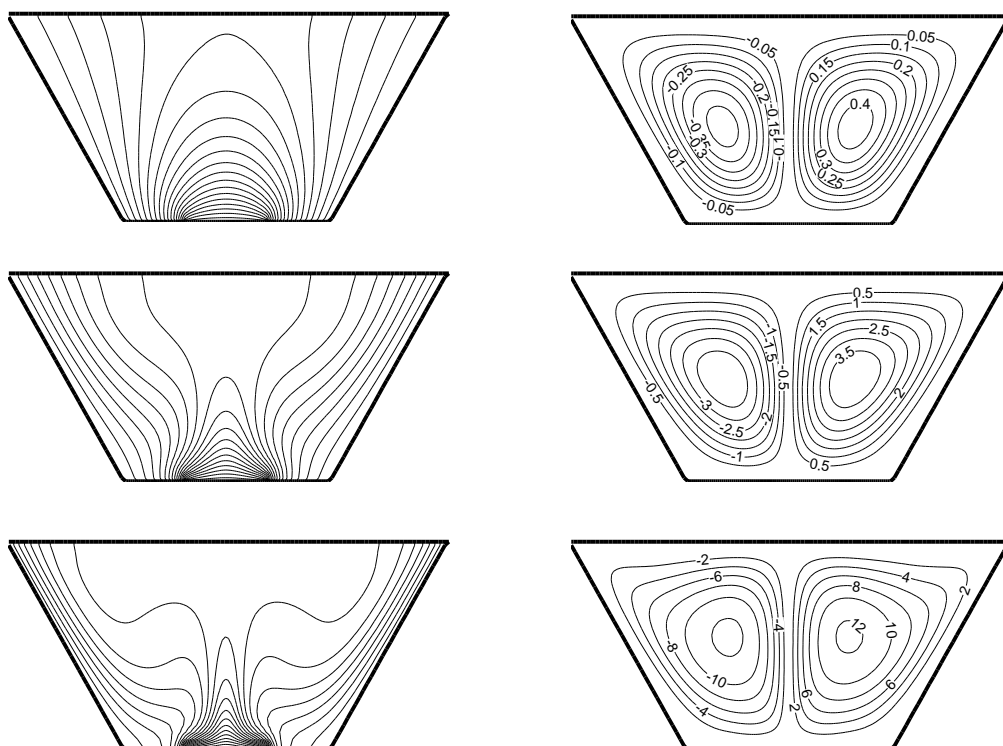


Fig.5. Isotherms (left) and Streamlines (right) for  $e = 2/5$  and (a)  $Ra = 10^3$  , (b)  $Ra = 10^4$  , (c)  $Ra = 10^5$ .

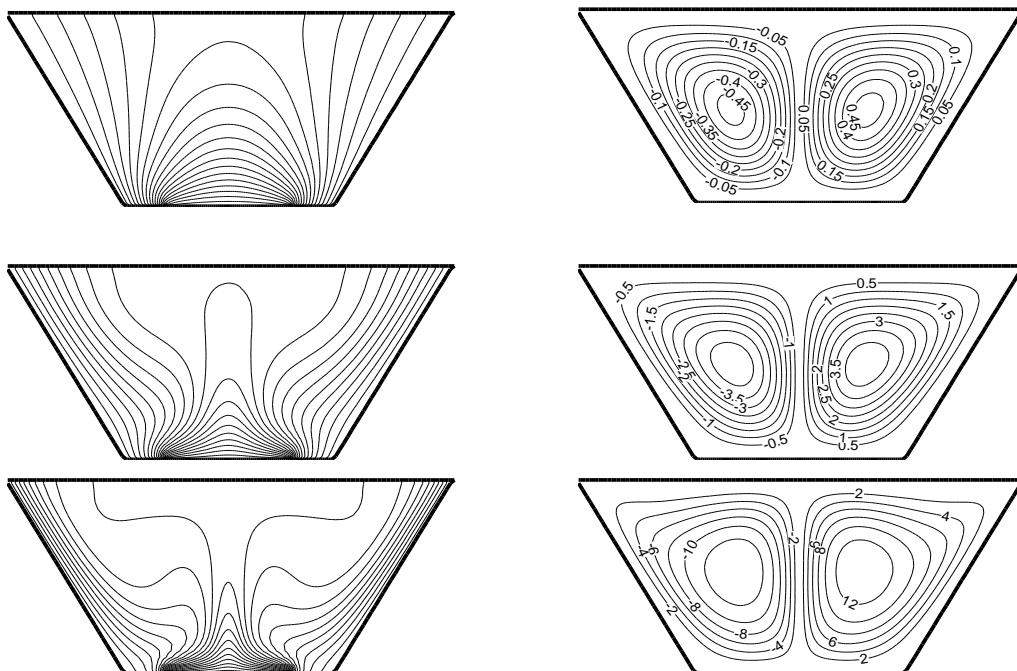


Fig.6. Isotherms (left) and Streamlines (right) for  $e = 3/5$  and (a)  $Ra = 10^3$  , (b)  $Ra = 10^4$  , (c)  $Ra = 10^5$

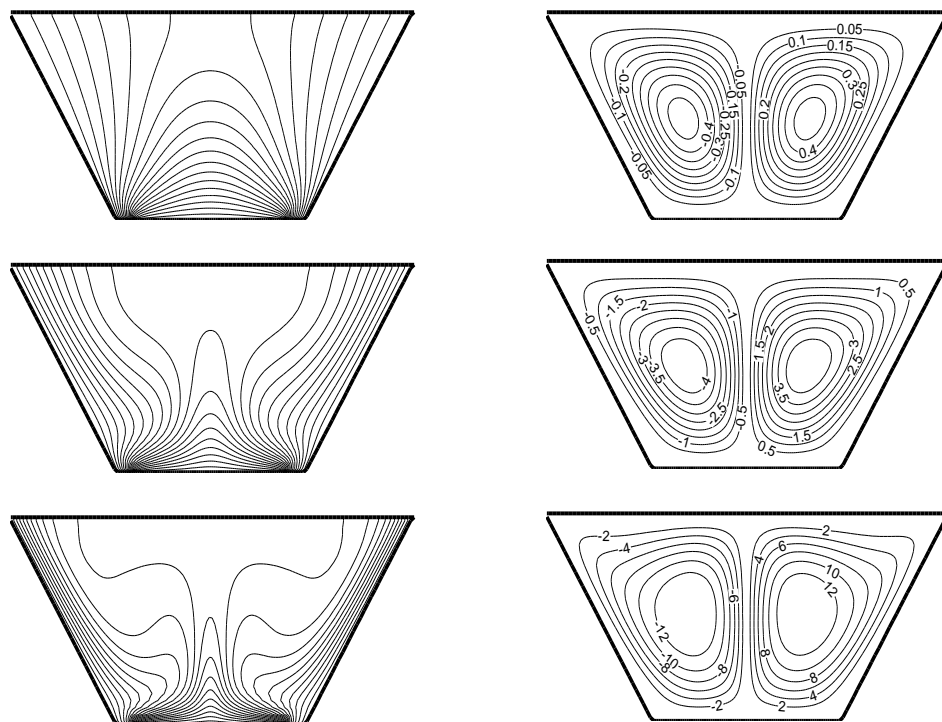


Fig.7. Isotherms (left) and Streamlines (right) for  $e = 4/5$  and (a)  $Ra = 10^3$  , (b)  $Ra = 10^4$  , (c)  $Ra = 10^5$ .

### 7.1. Effect of Rayleigh Number

Figure 4(a-c) shows the streamlines and isotherms pattern obtained for ( $e = 1/5$ ). For  $Ra = 10^3$ , the circulation inside the enclosure is so weak that the viscous forces are dominant over the buoyancy force. At  $Ra = 10^4$  the intensity of the circulation inside the enclosure increases as shown in (Figure 4b).

As Rayleigh number increases to  $10^5$ , the buoyancy driven circulation inside the cavity also increases as seen from greater magnitudes of the stream functions (Fig. 4c). It is interesting to observe that the stream function contours near the walls tend to have neck formation due to stronger circulation at higher Ra which contrasts the circulation patterns at smaller Ra as seen in (Fig. 4a). Due to stronger circulation, the isotherms are compressed near the middle portion of the vertical walls. Consequently, at  $Ra = 10^5$ , the temperature gradients near both the bottom and side walls tend to be significant to develop the thermal boundary layer. Due to greater circulation near the central core at the top half of the enclosure, there are small gradients in temperature at the central regime whereas a large stratification zone of temperature is observed at the vertical symmetry line due to stagnation of flow. The thermal boundary layer develops partially above the source for  $Ra = 10^3$  whereas for  $Ra = 10^5$ , the isotherms presented in (Fig. 4c) indicate that the thermal boundary layer develops almost throughout the entire source.

### 7.2. Effect of the Source Size

Streamlines and isotherms for  $e = 2/5, 3/5$ , and  $4/5$  at different Rayleigh numbers are seen in Figures 5, 6, and 7 respectively. The flow fields are nearly identical to those of ( $e = 1/5$ ) for each Rayleigh number. However, the isotherms are effected by the increasing of ( $e$ ) due to the heated part of the lower surface which is larger than that of ( $e = 1/5$ ), the heating effect in this case is much more sensible for the same values of Rayleigh numbers. For fixed Ra, with increasing ( $e$ ), the flow field remains almost the same, while the temperature fields changes become more stratified for larger values of Ra.

### 7.3. Heat transfer rates: local and average Nusselt numbers

Owing to the symmetry in the temperature field, heat transfer is symmetrical with respect to

mid-length ( $x = L/2$ ), this is illustrated in Figure (8) which shows the local Nusselt number along the heat source for ( $e = 4/5$ ) for different Rayleigh numbers.

The heat transfer rate (Nu) is very high at the edges of the source due to the discontinuities present in the temperature boundary conditions at the edges and reduces towards the center of the bottom wall with the minimum value at the center due to the plume formation at the center of the source.

Plots of the average Nusselt number on the heated source as a function of (Ra) and ( $e$ ) are shown in Figure 9. For a fixed ( $e$ ), increasing Ra enhances convection. And increasing ( $e$ ) for a fixed (Ra) results in an increase at Nusselt number. These results can be clearly explained under the views of isotherms given in Figures 4, 5, 6, and 7

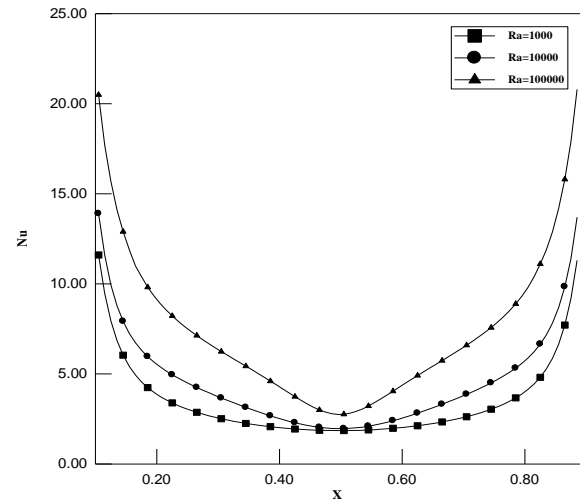


Fig.8. Local Nusselt Number on the Bottom Wall of the Enclosure for  $Ra = 10^5$ ,  $Pr=0.7$  and for ( $e = 4/5$ ).

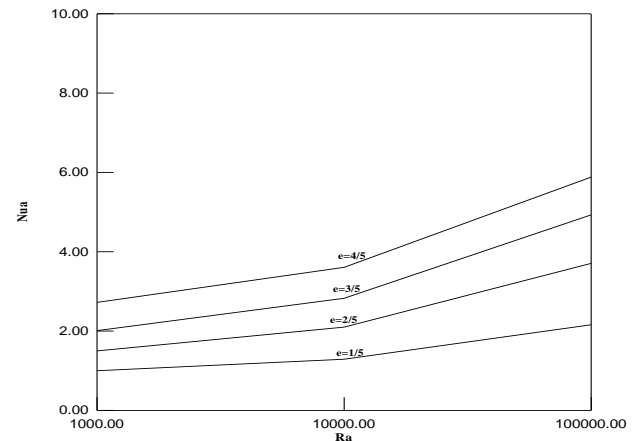


Fig.9. Average Nusselt Number Versus Rayleigh Number for three Different Values e.

## 8. Conclusions

The finite volume method with collocated grid is used to analyze the natural convection in trapezoidal enclosure heated partially from below. The heat transfer rates have been analyzed with local and average Nusselt numbers for the bottom wall of the enclosure. The results show

- 1- The average Nusselt number increases with increases of the source length.
- 2- The local Nusselt number is symmetrical with respect to mid- length for different source lengths and different Raleigh numbers

## Nomenclature

$C_1$	Contravariant velocity in $\zeta$ direction
$C_2$	Contravariant velocity in $\eta$ direction
$g$	gravitational acceleration, $m/s^2$
$H$	Dimensionless enclosure height
$J$	Jacobian transformation
$k$	Thermal conductivity, $W/m K$
$L$	Enclosure width
$Nu$	Nusselt number = $hL/k$
$p$	Pressure(Pa)
$P$	Dimensionless pressure
$Pr$	Prandtl number, $cp \mu/k$
$Ra$	Rayleigh number
$E$	Heat source length
$e$	Dimensionless heat source length
$T$	Temperature, $K$
$u, v$	Velocity components in the x and y direction, $m/s$
$U, V$	Dimensionless velocity components in and Y directions
$x, y$	Space coordinates in Cartesian system
$X, Y$	Dimensionless cartesian coordinates
$S_\phi$	Source term

## Greek Symbols

$\beta$	Coefficient of volumetric thermal expansion, $K^{-1}$
$\alpha, \beta, \gamma$	Dimensionless coordinate transformation parameters

$\Gamma$	Dimensionless diffusion coefficient
$\theta$	Dimensionless temperature
$\nu$	Kinematic viscosity, $m^2/s$
$\rho$	Density $kg /m^3$
$\zeta, \eta$	Dimensionless curvilinear coordinates
$\Phi$	Dimensionless dependent variable
$\phi$	Angle

## Subscripts

$c$	cold surface
$h$	hot surface

## 9. References

- [1] Iyican L., Bayazitoglu Y., An analytical study of natural convective heat transfer within trapezoidal enclosure, ASME J. Heat Transfer 102 (1980) 640–647.
- [2] Peric' M., Natural convection in trapezoidal cavities, Numer. Heat Transfer A 24 (1993) 213–219.
- [3] Kuyper, R.A. Hoogendoorn, C.J. "Laminar natural convection flow in trapezoidal enclosures", Num. Heat Transfer, Part A 28 (1995) 55–67.
- [4] Natarajan E., Tanmay Basak, and Roy S., Natural convection flows in a trapezoidal enclosure with uniform and non-uniform heating of the bottom wall, Int. J. Heat Mass Transfer, 51, 747–756, 2008.
- [5] Basak T., Roy S., and Pop I., Heat flow analysis for natural convection within trapezoidal enclosures based on heatline concept, Int. J. Heat Mass Transfer 52, 2471–2483, 2009
- [6] Bejan A., "Heat Transfer", John Wiley and Sons, 1993.
- [7] Thompson, J.F., Warsi, Z.U.A., and Mastin, C.W., Numerical Grid Generation, Foundations and Applications. Elsevier, New York 1985.
- [8] Rhie, C. M., and Chow, W. L., Numerical Study of the Turbulent Flow Past an Airfoil with Trailing Edge Separation, AIAA Journal, 21, 1525-1532, 1983.
- [9] Wang Y. and Komori S., On the improvement of the SIMPLE-like method for

- flows with complex geometry, *Heat and Mass Transfer* 36, 71-78, 2000.
- [10] Ferziger, J.H. and Peric, M. *Computational Methods for Fluid Dynamics*, Springer 1996.
- [11] Aydin, O. and Yang W., Natural Convection in Enclosures with Localized Heating from Below and Symmetrical Cooling from Sides, *Int. J. of numerical methods for Heat and fluid flow*, Vol. 10, No. 5, 518–529, 2000.

## الحمل الحر في حيز شبة منحرف مسخن جزئيا من الاسفل

أحمد وحيد مصطفى\* أحسان علي غني\*\*

\* قسم الهندسة الميكانيكية/ كلية الهندسة / جامعة تكريت

\*\* قسم الهندسة الميكانيكية/ كلية الهندسة/ الجامعة المستنصرية

\* البريد الإلكتروني: [ahmedweh@yahoo.com](mailto:ahmedweh@yahoo.com)

\*\* البريد الإلكتروني: [iaghani68@yahoo.com](mailto:iaghani68@yahoo.com)

### الخلاصة

الحمل الحر في حيز شبه منحرف مع تسخين جزئي من الاسفل وتبريد متناظر من الجوانب تم دراسته عدديا. التسخين تم تمثيلة بواسطة مصدر حراري موضوع على مركز الجدار السفلي اربع قيم مختلفه من طول المصدر هي (1/5, 2/5, 3/5, 4/5) تم اعتبارها في الدراسة. حقل الجريان الطبقي تم تحليله عدديا بحل معادلات نافير ستوك والطاقة الثنائي البعد وللحالة المستقرة. مركبات السرعة الدكارتية والضغط على شبكة متحدة الموقع استخدمت كمتغيرات متعمدة في معادلة الزخم التي تم تقطيعها باستخدام طريقة الحجم المحدد. نظام تطابق الاحداثيات استخدم لتمثيل شكل الحيز بشكل دقيق، تم توليد شبكة الحل العددي بحل معادلات تفاضلية جزئية ببيضوية. خوارزمية SIMPLE استخدمت لتحقيق حفظ الكتلة. مدى رقم راييلي هو ( $10^3 \leq Ra \leq 10^5$ ). النتائج بينت ان متوسط رقم نسلت يزداد بزيادة طول المصدر.